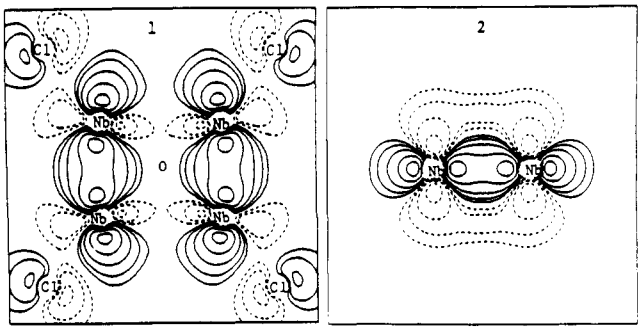

Figure 6. Contour plots for the $13a_g$ orbital in $[Nb_4OCl_8(C_4H_4)_2]^{2-}$ with the same contour values as in Figure 5.

considered as a consequence of the alternating Nb–Nb-bonded and $Nb(\mu\text{-}Cl)_2Nb$ edges.

Nb–Nb Bonding. It was previously[4] suggested, in purely qualitative terms, that by regarding the $(CPh)_4$ ligand as formally dinegative and consisting of two halves each of which serves as a 3-electron bridging ligand (like Cl^-), the two halves of the $[Nb_4OCl_8\{(PhC)_4\}_2]^{2-}$ ion could be regarded as face-sharing bioctahedra that share the bridging Cl atoms and the central oxygen atom. On this basis, the niobium atoms have a formal oxidation number of III and the Nb–Nb bonds are double bonds. Let us now see whether the calculations provide any support for this suggestion.

We begin by looking for orbitals that are mainly metal atom based and localized between or across the pairs of metal atoms that form the short edges of the Nb_4 rectangle. We find two such orbitals, $11b_{2u}$ and $13a_g$, which have 83% and 73% metal contributions, respectively. Contour diagrams of the $13a_g$ orbital are shown in Figure 6 and the $11b_{2u}$ orbital has a very similar appearance except that the major lobes are negative on one side and positive on the other, instead of positive on both as in Figure 6. In each MO the major contributions are from overlaps between $d_{x^2-y^2}$ orbitals supplemented by a little d_{xz} character. Clearly, these two orbitals, each containing two electrons, constitute the MO equivalent of two strong Nb–Nb σ bonds.

However, there are no other orbitals that are also of clear and simple Nb–Nb bonding character. Additional Nb–Nb π bonding could be assumed to occur because of the shortness of the distance, 2.61 Å, but it must be distributed over several MOs and mixed with the bonding between the Nb atoms and the $(PhC)_4$ bridging units. The situation may be compared with a similar case in the diniobium complex $Nb_2Cl_4O(PhCCPh)(THF)_4$.[1,3] Our calculation[3] indicated that a full strength Nb–Nb π bond in this molecule can hardly be expected, and the relatively short Nb–Nb distance, 2.74 Å, can be considered to be the result of the strong binding of the $(PhC)_2$ unit to the Nb dimer. It is clear that the bonding interaction of the $(PhC)_4$ unit with the pair of Nb atoms in the tetramer is much stronger than the Nb–C bonding in the dimer. Therefore, the short Nb–Nb distance in the tetramer may be mainly attributed to the $(PhC)_4$ bridge strongly binded to the close pair of Nb atoms, in addition to the strong σ bond. On the other hand, it still seems reasonable, from the Nb–C bonding scheme discussed earlier, to regard the metal atoms as being effectively in formal oxidation states of III.

Acknowledgment. We thank The Robert A. Welch Foundation for support under Grant No. A-494.

Contribution from the Departments of Chemistry, North Carolina State University, Raleigh, North Carolina 27695-8204, and Clemson University, Clemson, South Carolina 29634-1905

Role of the LUMO in Determining Redox Stability for 2,3-Dipyridylpyrazine- and 2,3-Dipyridylquinoxaline-Bridged Ruthenium(II) Bimetallic Complexes

J. B. Cooper,† D. B. MacQueen,‡ J. D. Petersen,‡ and D. W. Wertz*,†

Received November 21, 1989

The cyclic voltammograms (CV) of $[Ru(bpy)_2]_2dpq^{4+}$ and $[Ru(bpy)_2]_2dpp^{4+}$ (dpp = 2,3-dipyridylpyrazine, dpq = 2,3-dipyridylquinoxaline, bpy = 2,2′-bipyridine) indicate six reversible reductions for each species in *N,N*-dimethylformamide (DMF). The resonance Raman (RR), electronic, and ESR spectra indicate that the first two electrons enter a redox orbital (LUMO) that is bridging ligand localized, while the next four electrons enter bpy-localized orbitals. The RR and ESR data and the separation between the two bridging ligand reduction potentials are all consistent with a redox orbital that is predominantly localized on the quinoxaline portion of the ligand for $[Ru(bpy)_2]_2dpq^{4+}$ but involves both the pyridyl and pyrazine portions of the bridge in $[Ru(bpy)_2]_2dpp^{4+}$. The irreversibility of the CV for the doubly reduced dpp complex in CH_3CN is interpreted in terms of a bridging ligand rearrangement involving the pyridyl rings and a breaking of a Ru–N bond upon the addition of the second electron. The redox stability of the dpq complex is attributed to a polarization of the LUMO away from the pyridyl rings toward the fused benzo ring.

Introduction

Complexes of the type $[Ru(bpy)_2]_2BL^{4+}$ (where BL is a π-delocalized tetraimine bridging ligand and bpy is 2,2′-bipyridine) have recieved a great deal of attention recently.[1-20] Although bimetallic species offer the possibility of 2-photon excitation, double chelation of the $Ru(bpy)_2^{2+}$ moieties to the bridging ligand results in a strong perturbation on the bridging ligand π system, usually resulting in a decrease or loss of luminescence with respect to the monometallic species.[2,5,6,14-16] Special emphasis has been placed to relating this loss to the degree of metal–metal communication mediated by the bridging ligand, and interpretation of spectroscopic and electrochemical data has led to several theories regarding the degree of communication between metal centers in such complexes.[6,13-15]

†North Carolina State University.
‡Clemson University.

(1) Braunstein, C. H.; Baker, A. D.; Strekas, T. C.; Gafney, H. D. *Inorg. Chem.* **1984**, *23*, 857.
(2) Dose, E. V.; Wilson, L. J. *Inorg. Chem.* **1978**, *17*, 2660.
(3) Humziker, B.; Ludi, A. *J. Am. Chem. Soc.* **1977**, *99*, 7370.
(4) Ruminski, R. R.; Petersen, J. D. *Inorg. Chem.* **1982**, *21*, 3706.
(5) Rillema, D. P.; Mack, K. B. *Inorg. Chem.* **1982**, *21*, 3849.
(6) Petersen, J. D. In *Supramolecular Photochemistry*; Balzani, V., Ed.; Reidel: Norwell, MA, 1987; p 135.
(7) Ernst, S.; Kaim, W. *Angew. Chem., Int. Ed. Engl.* **1985**, *24*, 430.
(8) Ernst, S.; Kaim, W. *J. Am. Chem. Soc.* **1986**, *108*, 3578.
(9) Kaim, W.; Kohlman, S. *Inorg. Chem.* **1987**, *26*, 68.
(10) Ernst, S.; Kaim, W. *Inorg. Chem.* **1989**, *28*, 1520.
(11) De Cola, L.; Barigelletti, F. *Gazz. Chim. Acta* **1988**, *118*, 417.
(12) Campagna, S.; Denti, G.; DeRosa, G.; Sabatino, L.; Ciano, M.; Balzani, V. *Inorg. Chem.* **1989**, *28*, 2565.
(13) Sahai, R.; Morgan, L.; Rillema, P. *Inorg. Chem.* **1988**, *27*, 3495.

0020-1669/90/1329-3701$02.50/0

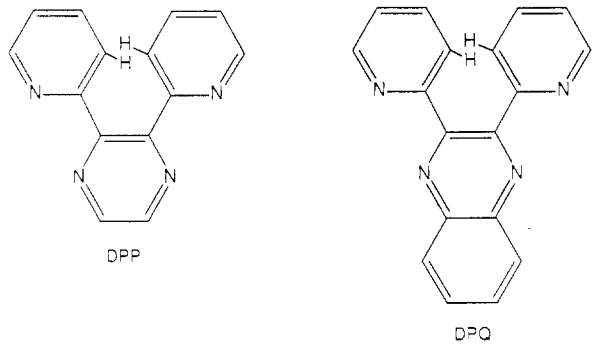

Figure 1. 2,3-Dipyridylpyrazine (dpp) and 2,3-dipyridylquinoxaline (dpq).

Table I. $E_{1/2}$ (V vs SCE) of the $[Ru(bpy)_2]_2BL^{m/n}$ Redox Couple

$E_{1/2}$			
BL = dpq	BL = dpp	m/n	assignt
+1.68	+1.61	+6/+5	Ru(II/III)[b]
+1.50	+1.41	+5/+4	Ru(II/III)[b]
-0.37	-0.69	+4/+3	BL/BL^{-}[b]
-1.15	-1.19[c]	+3/+2	BL^{-}/BL^{2-}[b]
~-1.4[a]	~-1.4[a,c]	+2/+1	BPY/BPY^{-}
~-1.5[a]	~-1.5[a,c]	+1/0	BPY/BPY^{-}
-1.70	-1.73[c]	0/-1	BPY/BPY^{-}
-1.82	-1.86[c]	-1/-2	BPY/BPY^{-}

[a] Due to overlap of the third and fourth waves, the exact $E_{1/2}$ values could not be determined. [b] Previously assigned.[1,5] [c] In DMF, all others in acetonitrile (0.1 M TBAH).

In this study, we present two bimetallic species bridged by the geometrically similar ligands 2,3-dipyridylpyrazine (dpp) and 2,3-dipyridylquinoxaline (dpq) shown in Figure 1. The dpp species is a strong emitter with an appreciable lifetime (τ = 134 ns, in fluid solution at room temperature), while the dpq bimetallic complex exhibits a much weaker emission with a lifetime <20 ns.[6] The fused benzo ring must be responsible for these differences in the emissive properties, and this paper presents a detailed spectroscopic and electrochemical study on the effect of the fused ring on the nature of the LUMO in the series $[Ru(bpy)_2]_2BL^{+(4-n)}$ (BL = dpp or dpq, n = 0–6).

Experimental Section

Chemicals. Anhydrous, 99+% *N,N*-dimethylformamide (DMF) and anhydrous, 99+% acetonitrile were purchased from Aldrich. Both solvents were stored in a drybox under nitrogen atmosphere, and the acetonitrile was dried on an alumina column prior to use. The dpp free ligand was purchased from Aldrich. The dpq free ligand was prepared and purified by the method of Goodwin et al.[21] $[Ru(bpy)_2]_2dpq(PF_6)_4$ and $[Ru(bpy)_2]_2dpp(PF_6)_4$ were prepared as previously published.[1,5] Both complexes were purified on a 20 × 2.5 cm neutral alumina column with a 2:1 acetonitrile–methanol eluent. Tetrabutylammonium hexafluorophosphate (TBAH) was purchased from Aldrich, recrystallized twice from ethanol, and dried under vacuum.

Electrochemistry. A solution of the bimetallic complex (1 mM) for ESR and RRS and 0.5 mM for UV/vis) and TBAH (100 mM) was prepared in a Vacuum Atmospheres Co. drybox under nitrogen atmosphere. The solution was loaded into an electrochemical H-cell with Pt-mesh working and counter electrodes referenced to a saturated calomel electrode (SCE). The cyclic voltammograms were collected digitally by using a Nicolet Model 3091 digital oscilloscope connected to a Hokuto Denko Model HA-211A potentiostat and Model HB-111 function generator. The digitized data was downloaded to an AT&T PC 6300 computer. The extent of reduction was monitored with an in-line PAR Model 379 digital coulometer. The procedures and equipment used in the resonance Raman and UV/vis experiments have been described previously.[22] In the ESR experiments, the reductions were carried out in the drybox and the solutions were transferred to Suprasil quartz ESR cells, which were placed in an IBM-Bruker Series 200 spectrometer.

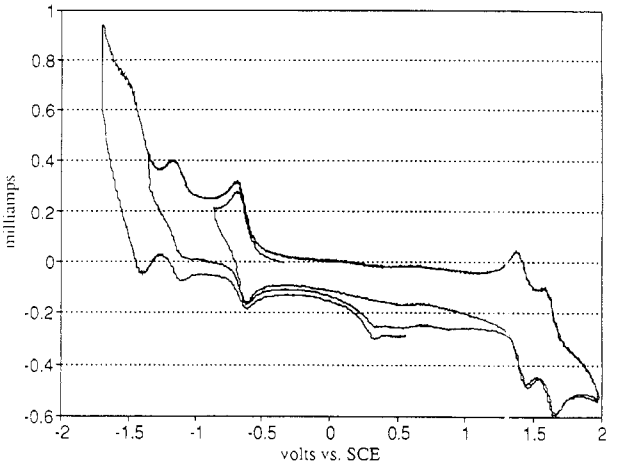

Figure 2. Cyclic voltammogram of $[Ru(bpy)_2]_2dpp^{4+}$ in CH_3CN with 0.1 M TBAH at 200 mV/s.

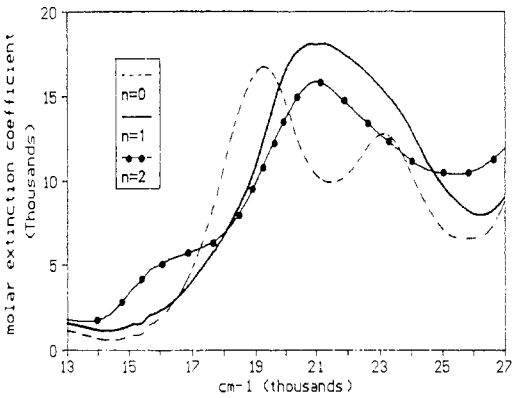

Figure 3. Visible region of the electronic spectra of $[Ru(bpy)_2]_2dpp^{+(4-n)}$ (n = 0, 1, 2), where n indicates the number of redox electrons added and ϵ is the extinction coefficient in $dm^3\ mol^{-1}\ cm^{-1}$.

Results and Assignments

Electrochemistry. The oxidation and reduction potentials for both complexes are given in Table I. The oxidations at +1.50 and +1.68 V for the dpq complex and +1.41 and +1.61 V for the dpp complex have been previously assigned as the two Ru(II/III) couples. In addition, the first two reductions for both complexes have been assigned as reductions of the bridging-ligand-centered LUMO.[1,5] Our resonance Raman data for the reduced species is in agreement with these assignments. At more negative potentials, there are four more reductions, which, on the basis of changes in the UV portion of the electronic spectra for the bulk reduced species (see discussion of electronic spectra), can be assigned as one-electron bipyridine-centered reductions. This gives a total of six one-electron reductions for each complex. For both complexes, bulk electrolysis in DMF at any of these potentials and subsequent reoxidation results in the original CV. This, along with the ~60 mV peak to peak separation of the anodic and cathodic waves for each couple, indicates that all six redox processes are reversible. The CV for $[Ru(bpy)_2]_2dpp^{4+}$ in acetonitrile is shown in Figure 2. If the CV is reversed after the first redox couple, the process appears reversible. However, if the CV is scanned past the second redox wave and reversed, an oxidative

(14) Fuchs, Y.; Sonita, L.; Dieter, T.; Shi, W.; Morgan, R.; Strekas, T.; Gafney, H.; Baker, D. *J. Am. Chem. Soc.* **1987**, *109*, 2691.
(15) Hosesk, W.; Tysoe, S.; Gafney, H.; Baker, D.; Strekas, T. *Inorg. Chem.* **1989**, *28*, 1228.
(16) Knorrs, C.; Gafney, H.; Baker, D.; Braunstein, C.; Strekas, T. *J. Raman Spectrosc.* **1983**, *14*, 32.
(17) Barigelletti, F.; Juris, A.; Balzani, V; Belser, P.; von Zelewsky, A. *Inorg. Chem.* **1987**, *26*, 4115.
(18) Juris, A.; Balzani, V.; Barigelletti, F.; Campagna, S.; Belser, P.; von Zelewsky, A. *Coord. Chem. Rev.* **1988**, *84*, 85.
(19) Kalyanasundaram, K.; Nazeeruddin, Md. K. *Chem. Phys. Lett.* **1989**, *158*, 45.
(20) Kirsche-De Mesmaeker, A.; Jacquet, L.; Masschelein, A.; Vanhecke, F.; Heremans, K. *Inorg. Chem.* **1989**, *28*, 2465.
(21) Goodwin, H. A.; Lions, F. *J. Am. Chem. Soc.* **1959**, *81*, 6415.
(22) Cooper, J. B.; Wertz, D. W. *Inorg. Chem.* **1989**, *28*, 3108.

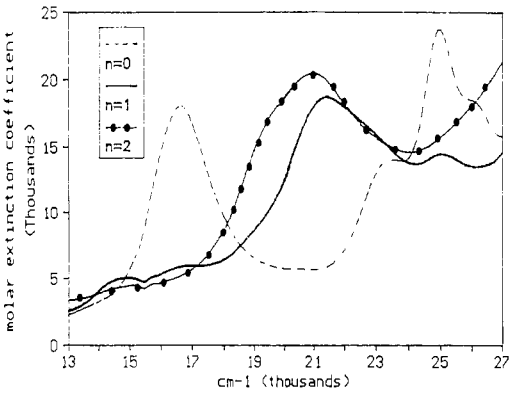

Figure 4. Visible region of electronic spectra of $[Ru(bpy)_2]_2dpq^{+(4-n)}$ (n = 0, 1, 2), where n indicates the number of redox electrons added and ϵ is the extinction coefficient in $dm^3\ mol^{-1}\ cm^{-1}$.

process grows in at +0.4 V. The anodic current at +0.4 V increases as the CV is scanned to even more negative potentials and reversed. Bulk electrolysis past the second redox wave results in significant degradation of the CV. In order to elucidate the nature of this irreversibility in acetonitrile as opposed to DMF, a strongly coordinating ligand (CN^-) was added to the DMF at the same concentration as the sample. The CV remained unperturbed if reversed after the first redox wave, but if scanned past the second redox wave and then reversed, the CV showed signs of irreversibility with new oxidation waves growing in at −0.2 V at +0.4 V. The nature of this irreversibility will be discussed later in the text.

Electronic Spectra. The $[Ru(bpy)_2]_2dpp^{+(4-n)}$ complex has only two bands in the visible (Figure 3) at 19.3×10^3 and 23.2×10^3 cm^{-1} which have been assigned by Knorrs et al.[16] to metal-to-ligand charge transfers (MLCT) into the dpp and bpy, respectively in the $n = 0$ species. For the $n = 1$ species, a peak is observed at 21.0×10^3 cm^{-1} with a shoulder at $\sim 23 \times 10^3$ cm^{-1}. With the addition of a second electron, it appears that the main peak is unshifted but the high-energy shoulder disappears and a low-energy shoulder near 16×10^3 cm^{-1} appears. Other studies[23-25] have indicated that, upon reduction of one ligand, the MLCT into an unreduced bpy red-shifts and redox orbital based $\pi^* \rightarrow \pi^*$ transitions often appear in the visible region. Resonance Raman data obtained by using excitation near 21×10^3 cm^{-1} for both the $n = 1$ and $n = 2$ species yielded only the typical bipyridine spectrum and no evidence for the reduced ligand. Our Raman system is unable to probe higher than 21.8×10^3 cm^{-1} so the high-energy shoulder ($n = 1$) could not be studied. When the low-energy shoulder ($n = 2$) was investigated, a very weak bpy spectrum was again observed, but the strongest nonsolvent mode in the spectrum is at 1462 cm^{-1}; this frequency does not correspond to a bpy mode and is assigned to a dpp^- mode. On the basis of these observations, we assign the 21.0×10^3 cm^{-1} peak to the Ru → bpy MLCT, which red shifts 2.0×10^3 cm^{-1} upon reduction (resulting from a shutting off of $d\pi$ back-donation into the BL) and remains at essentially the same energy upon a second reduction. The high-energy shoulder found at 23×10^3 cm^{-1} for $n = 1$ is then tentatively assigned as a dpp-based $\pi^* \rightarrow \pi^*$ transition involving the redox electron that red shifts 6.6×10^3 cm^{-1} (to 16×10^3 cm^{-1}) when the second electron is added.

The visible portion of the spectrum of $[Ru(bpy)_2]_2dpq^{4+}$ as shown in Figure 4 has four peaks (16.6×10^3, 23.4×10^3, 25.0×10^3, and 26.1×10^3 cm^{-1}). On the basis of resonance Raman results (vida infra) the 16.6×10^3 cm^{-1} band is readily assigned as the Ru → dpq charge transfer. The intensity and position of the 23.4×10^3 cm^{-1} band argue for its assignment to the Ru → bpy MLCT (same energy and ϵ as for the dpp complex). The remaining bands are then tentatively assigned as Ru → dpq SLUMO at 25.0×10^3 cm^{-1} with a vibronic side band at 26.1×10^3 cm^{-1}. $[Ru(bpy)_2]_2dpq^{+(4-n)}$ ($n = 1, 2$) behaves much the same as its dpp analogue with a moderately strong band centered at $\sim 21 \times 10^3$ cm^{-1} with shoulders at 25.1×10^3 and 23×10^3 cm^{-1} ($n = 1$) and 19.5×10^3 cm^{-1} ($n = 2$). On the basis of the assignments in this region for dpp, the 21.3×10^3 cm^{-1} peak ($n = 1$) is assigned to Ru → bpy MLCT (red-shifted 2000 cm^{-1}) with the shoulders arising from a $dpq^- \pi^* \rightarrow \pi^*$. RRS using 19.4×10^3 cm^{-1} excitation yielded no evidence for the dpq^- species, but reduced ligands have been shown to gain very little enhancement in the visible region.[23-25] One explanation of this lack of enhancement would be that the $\pi^* \rightarrow \pi^*$ transition results in little excited state displacement; i.e., the bridging ligand LUMO and SLUMO must be very similar. Recent studies in our laboratory have shown that for $[Ru(bpy)_2]_2(tppq)^{4+}$ (tppq = 2,3,7,8-tetrakis(2-pyridyl)pyrazino[2,3-g]quinoxaline—essentially a dpp and a dpq fused together), the resonance Raman spectra when probing the MLCT transitions into the bridging ligand LUMO and SLUMO are almost identical, indicative of the similarity of the two excited states.[26] The assignments of the visible region of the electronic spectra of both complexes are summarized in Table II.

Table II. Electronic Spectral Data ($\bar{\nu}$, $cm^{-1} \times 10^{-3}$, DMF 0.1 M TBAH) and Assignments

	$\bar{\nu}$			
	$n = 0$	$n = 1$	$n = 2$	assignt
$[Ru(bpy)_2]_2dpp^{+(4-n)}$	19.3[b]			MLCT (Ru → BL LUMO)
	23.2[b]	21.0[a]	21.0[a]	MLCT (Ru → BPY LUMO)
		23.0	16.0[a]	BL $\pi^* \rightarrow \pi^*$
$[Ru(bpy)_2]_2dpq^{+(4-n)}$	16.6[c]			MLCT (Ru → BL LUMO)
	23.4[c]	21.3[a]	21.5[a]	MLCT (Ru → BPY LUMO)
		23.0		vibronic
	25.0			MLCT (Ru → BL SLUMO)
	26.1			vibronic
		25.1	19.5[a]	BL $\pi^* \rightarrow \pi^*$

[a] Assignments are based on RR data; other assignments are speculative. [b] Previously assigned.[1,14,16] [c] Previously assigned.[5]

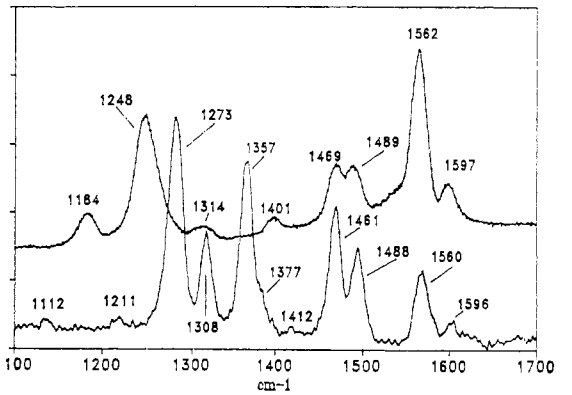

Figure 5. Resonance Raman spectra of $[Ru(bpy)_2]_2dpp^{4+}$ (19 400-cm^{-1} excitation) in H_2O (top) and of $[Ru(bpy)_2]_2dpq^{4+}$ (16 600-cm^{-1} excitation) in CH_3CN (bottom).

(23) Donohoe, R. J.; Tait, C. D.; DeArmond, M. K.; Wertz, D. W. *Spectrochim. Acta* **1986**, *42*, 233. Donohoe, R. J.; Tait, C. D.; DeArmond, M. K.; Wertz, D. W. *J. Phys. Chem.* **1986**, *90*, 3923.
(24) Tait, C. D.; Donohoe, R. J.; DeArmond, M. K.; Wertz, D. W. *Inorg. Chem.* **1987**, *26*, 2754.
(25) Tait, C. D.; MacQueen, D. B.; Donohoe, R. J.; DeArmond, M. K.; Hanck, K. W.; Wertz, D. W. *J. Phys. Chem.* **1986**, *90*, 1766.
(26) Kalsbeck, W. A.; Cooper, J. B.; Wertz, D. W. Work in progress.
(27) Brandt, W.; Dwyer, F.; Gyarbar, E., *Chem. Rev.* **1954**, *54*, 959.
(28) Hanazaki, I.; Nagakura, S. *Inorg. Chem.* **1969**, *8*, 648.
(29) Krumbolz, P. *J. Am. Chem. Soc.* **1953**, *75*, 2163.
(30) Palmer, R.; Piper, T. *Inorg. Chem.* **1966**, *5*, 864.
(31) Bryant, G.; Ferguson, J.; Powell, H. *Aust. J. Chem.* **1971**, *24*, 257.
(32) Gex, J. N.; Brewer, W.; Bergmann, K.; Tait, C. D.; DeArmond, M. K.; Hanck, K. W.; Wertz, D. W. *J. Phys. Chem.* **1987**, *91*, 4776. Gex, J. N.; Cooper, J. B.; Hanck, K. W.; DeArmond, M. K. *J. Phys. Chem.* **1987**, *91*, 4686. Morris, D. E.; Hanck, K. W.; DeArmond, M. K. *J. Am. Chem. Soc.* **1983**, *105*, 3032.

Table III. Comparison of the RRS Wavenumbers (cm^{-1}) for $[Ru(bpy)_2]_2dpq^{4+}$ to Those Observed in the SERS of Quinoxaline (quin)[36]

quin SERS	dpq RRS	quin SERS	dpq RRS
1014	1025	1350	1357
1039	1038	1375	1377
1075	1061	1418	1412
1102	1112	1450	1461
1201	1211	1496	1488
1268	1273	1575	1560
1298	1308		1596

The UV region of the electronic spectra for $[Ru(bpy)_2]_2dpp^{+(4-n)}$ (n = 2–6) is similar to that reported for other of Ru–bipyridine complexes and consists of a strong band near 35×10^3 cm^{-1}, which is assigned to a bipyridine-based $\pi \rightarrow \pi^*$ transition. With each successive reduction, there is a monotonic decrease in the intensity of this band supporting the assignment of the last four redox waves as bpy-localized reductions.[23-25] The same monotonic decrease occurs with further reduction of the dpq complex, also implying bpy-localized reductions. With each addition of an electron there is also a successive growth centered at 28×10^3 cm^{-1} arising from $\pi^* \rightarrow \pi^*$ transitions involving the bpy-localized redox electrons.[23-25]

Resonance Raman Spectra. The resonance Raman spectra (RRS) observed for $[Ru(bpy)_2]_2BL^{4+}$ when exciting into the Ru $\rightarrow$ BL MLCT are shown in Figure 5 for BL = dpp (top) and dpq (bottom). On the basis of the enhancement of the "pyrazine-like" modes at 1248 and 1562 cm^{-1} in the RRS of the dpp complex, Knorrs et al.[16] suggest that the bulk of the charge transfer is into a pyrazine-based orbital. The RRS of the dpq and dpp complexes in this region are very similar, especially in the peak positions above 1400 cm^{-1}. Perhaps the most outstanding difference between the two spectra is the appearance of a very strong band at 1357 cm^{-1} with a shoulder at 1377 cm^{-1} in the RRS of dpq. Both of these bands appear as moderately strong peaks in the SERS study of the quinoxaline molecule (1350 and 1375 cm^{-1}).[36] Since there is a reasonably good correlation between the dpp and dpq spectra except for these two peaks, it is reasonable to assume that they involve considerable contributions from the fused ring. In addition, the 1273-cm^{-1} peak, the strongest in the spectrum, is also found in the SERS of quinoxaline at 1267 cm^{-1}. In fact, there is a one-to-one correspondence (with the exception of a very weak mode at 1596 cm^{-1}) between the SERS for quinoxaline and the RRS for dpq (see Table III). Although the frequencies and intensities of the SERS spectrum of the free ligand and those of the RRS spectrum of the metal-bound ligand are expected to differ, the agreement in number and position of peaks seems to indicate that almost all of the intensity of the dpq RRS can be attributed directly to quinoxaline vibrations. Thus the RRS of the dpq complex is consistent with a quinoxaline-localized optical orbital.

ESR Spectra. The room-temperature ESR spectrum for $[Ru(bpy)_2]_2dpq^{+3}$ is shown in Figure 6a. Previous studies have attributed a lack of resolved hyperfine splitting (hfs) in similar Ru–diimine complexes to spectral density.[23,33] Although the line widths for this dpq complex are very broad, implying unresolved hfs structure, an intense central five-line splitting pattern attributable to two equivalent nitrogen atoms (I = 1; a_N = 6.65 G) can be seen. The broad line widths as well as the shape of the envelope can be ascribed to additional splittings arising from at least one pair of equivalent hydrogen atoms ($I = {}^1/_2$) as well as satellites arising from the isotopic splitting of the two ruthenium metal centers ($I = {}^5/_2$). The most reasonable explanation for such a splitting pattern is one in which the redox orbital encompasses the quinoxaline portion of the bridging ligand. Bulk electrolysis at the second reduction potential results in an ESR-silent species at room temperature and 77 K, which for these species is usually indicative of electron pairing.

(33) Kaim, W.; Ernst, S.; Kohlmann, S.; Welkerling, P. *Chem. Phys. Lett.* **1985**, *118*, 431.

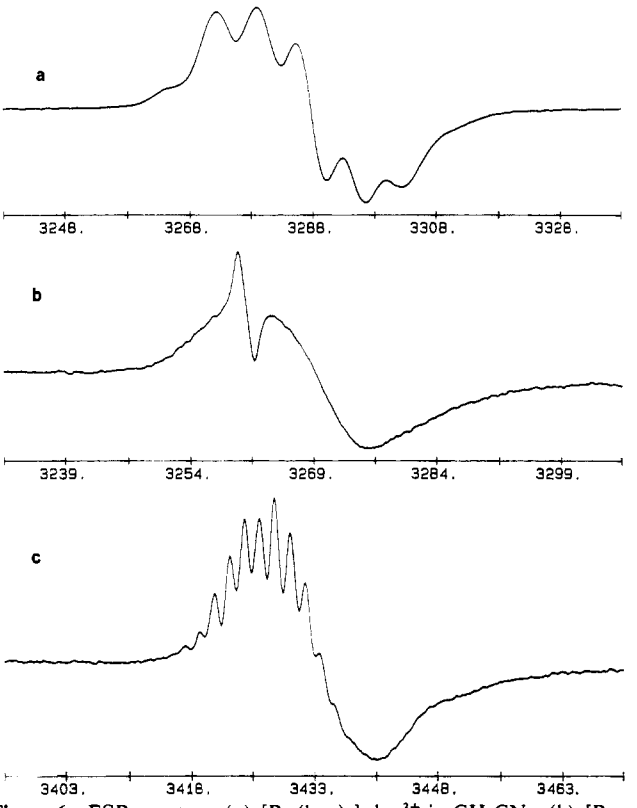

Figure 6. ESR spectra: (a) $[Ru(bpy)_2]_2dpq^{3+}$ in CH_3CN: (b) $[Ru(bpy)_2]_2dpp^{3+}$ (g = 2.00) in CH_3CN, with a small signal due to DPPH external standard; (c) $[Ru(bpy)_2]_2dpp^{2+}$ (g_{ef} = 2.00) in CH_3CN after exposure to O_2.

The ESR spectrum for $[Ru(bpy)_2]_2dpp^{+3}$ in DMF (Figure 6b) shows only a broad $s = {}^1/_2$ envelope. The loss of hfs for the dpp bridge with respect to the dpq bridge can only be justified by the introduction of additional nuclear splittings. If the redox orbital is confined solely to the pyrazine portion of the bridging ligand, it is difficult to rationalize the increase in spectral density since the quinoxaline portion of the dpq bridge has two additional protons. Loss of hfs due to introduction of additional nonequivalent nuclear splitting is quite reasonable if a portion of the dpp LUMO is on the pyridyl rings. The net effect would be an increased density of states resulting in an unresolved envelope.

Like the dpq bimetallic complex, the two-electron species is spin paired in DMF. Although the two-electron species in acetonitrile is also ESR silent, after it is exposed to oxygen, an ESR signal appears (Figure 6c). The resulting spectrum is obviously a composite of two signals (both stable in the presence of O_2), one of which shows some resolved hfs (a = 2.0 G). The signal displaying hfs cannot be fitted to either the reduced free ligand (which is not stable to O_2) or to a reduced $[Ru(bpy)_2]dpp$ moiety (which displays only a broad $s = {}^1/_2$ signal), thus eliminating liberation of the bridging ligand or a $Ru(bpy)_2^{2+}$ moiety. A likely alternative would be a species in which one of the Ru–N bonds is cleaved. The remaining broad ESR signal must then correspond to the singly reduced bimetallic dpp complex.

Discussion

The electrochemistry and spectroscopy (RRS and electronic) for $[Ru(bpy)_2]_2BL^{4+}$ (BL = dpp and dpq) all support a LUMO that is localized on the bridging ligand. In addition, ESR indicates that electron pairing occurs upon the second reduction, while the CV's and electronic spectra require that the next four redox processes involve sequential reduction of bpy-localized orbitals. The RRS of these bimetallic species show that the lowest energy optical transition results from a charge transfer from a metal $d\pi$ to a bridging-ligand-localized orbital. The ESR and RRS are consistent with redox and optical orbitals localized solely on the quinoxaline portion of the bridging dpq ligand. The ESR for the dpp complex, however, is indicative of some participation of the

pyridyl rings in the redox orbital.

The instability of the dpp bimetallic complex in acetonitrile to two-electron reduction is quite interesting when compared to the stability of the dpq bimetallic complex with up to six electron additions. The fact that two individual ESR signals are detected for the two-electron product after being exposed to oxygen is evidence for a bond breaking mechanism. On the basis of molecular models, it has been reported that the pyridyl rings on the dpp bridging ligand (and analogously dpq) must be nonplanar with respect to the pyrazine ring due to steric hindrance of the pyridyl hydrogens.[16] In fact, X-ray crystallographic data for $(bpy)_2Ru(dpp)Ir(bpy)_2(PF_6)_4$ indicates that the pyridyl–pyrazine twist angle (θ) on both the Ru and Ir bound sides is 19.5°.[34] MNDO calculations performed in our lab on the dpp free ligand indicate that the HOMO has considerable antibonding character between the pyridyl and pyrazine inter-ring carbons; i.e., the carbon p_z orbitals are out of phase. Thus the twist of the pyridyl rings from planarity not only removes the steric hindrance but also stabilizes the HOMO as the overlap between the carbon p_z orbitals decreases with $\cos^2\theta$. This is also supported by the X-ray crystallographic data on $Ir(dpp)(P(C_6H_5)_3)_2H_2$, indicating a twist angle of 53.8° for the unbound pyridyl ring and a twist angle of 17.9° for the bound pyridyl ring.[34] Even though the unbound pyridyl is free to rotate to remove the steric hindrance, the bound ring still twists to minimize the overlap and stabilize the HOMO. Since the ESR spectrum and the CV for the dpq complex do not show any sign of decomposition upon second reduction and since the RR and ESR spectra indicate that the dpq LUMO is quinoxaline based, it is reasonable to propose that the bond-breaking mechanism for the dpp complex involves a rearrangement of the pyridyl rings. Although the exact nature of the rearrangement is uncertain, it is likely that cleavage occurs as nucleophilic ligands (CH_3CN or CN^-) attack a Ru^{II} center at a strained Ru–pyridyl bond. In the case of the dpq bimetallic complex, the redox orbital is quinoxaline localized with little contribution from the pyridyl rings so that its energy is less dependent upon their orientation, thus giving the greater redox stability.

The energy associted with intra- and intermolecular reorganization (χ) can be related to the MLCT optical energy (E_{op}) and the electrochemical potentials as follows:[35] $E_{op} = [E_{ox} - E_{red}] + \chi$, where E_{ox} is the first oxidation potential of a Ru^{II} center and E_{red} is the reduction potential of the bridging ligand. For the dpq complex, the value calculated for χ is 0.19 eV while for the dpp complex it is calculated to be 0.29 eV. Since the solvation energies would be expected to be similar, the large difference is most likely due to a larger inner-sphere reorganization for the dpp bimetallic complex, presumably involving the pyridyl rings.

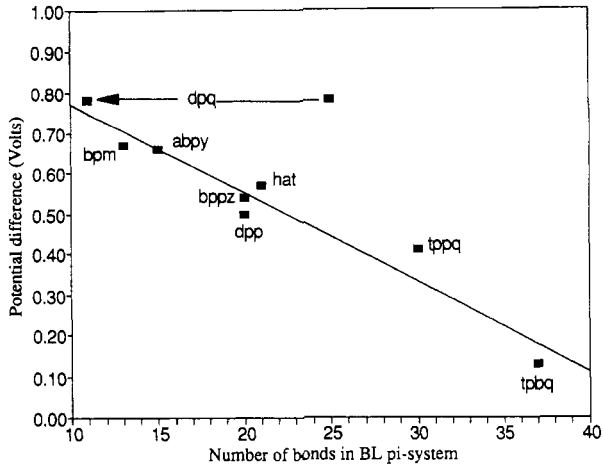

Figure 7. Plot of the potential difference for the first two reductions of BL vs the number of bonds in the BL π system for a series of $[Ru(bpy)_2]_2BL$ complexes. For tppq and tpbq, the two noncoordinating pyridyl rings were not included.[26] Linear regression: $R = 0.98$; intercept = 1.0 V; slope = −0.024 V/bond. abpy is azo-2-pyridine; bppz is 2,5-(2-pyridyl)pyrazine.[10] hat is benzo[1,2-*b*:3,4-*b*′:5,6-*b*″]tripyrazine; bpm is 2,2′-bipyrimidine.[37] tpbq is 2,2′,3,3′-tetrakis(2-pyridyl)-6,6′-biquinoxaline.[38] tppq is 2,3,7,8-tetrakis(2-pyridyl)pyrazino[2,3-*g*]quinoxaline.[5]

A further argument for a quinoxaline-based redox orbital in the dpq complex and for a redox orbital spread into the pyridines for the dpp complex can be made from the separation of the two bridging ligand reductions (0.50 V for dpp and 0.79 V for dpq). If the major contribution to this separation is due to a Coulombic repulsion between the electrons, then it follows that the smaller the π system into which the redox electron is added, the greater should be the separation between these two redox couples. On the basis of this consideration, it would appear that the dpp redox orbital is the larger. However, other factors like differing metal involvement and solvation and reorganization energies can also affect this separation. In order to elucidate the relative effect of these other factors and to test the feasibility of such simple considerations, the difference in these redox potentials for a series of $[Ru(bpy)_2]_2BL$ complexes have been tabulated and plotted versus the number of bonds in the π system (size). In compiling these data, we have attempted to include all complexes of the type $[Ru(bpy)_2]_2BL$ that have been reported to show reversible redox behavior. As can be seen in Figure 7, the relationship appears to be linear with only one deviation, BL = dpq. If however, only the 11 bonds of the quinoxaline portion are used rather than the 25 bonds of the entire system, then $[Ru(bpy)_2]_2dpq$ also falls on the line. For the dpp complex, however, the relationship is satisfied when the entire set of 20 bonds encompassing both the pyrazine and pyridine portions of the ligand are used. The relationship suggested here should be useful in the design of systems with specific sets of redox properties, and an interpretation of the slope and intercept based on a larger data base (both ligand and metal) would certainly aid in our understanding of redox orbitals.

(34) MacQueen, D. B.; Pennington, W. T.; Petersen, J. D. Submitted for publication.
(35) Dodsworth, E.; Lever, B. *Chem. Phys. Letts.* **1985**, *119*, 61.
(36) Takahashi, M.; Sakai, I., Fujita, M.; Ito, M.; *Surf. Sci.* **1986**, *176*, 351.
(37) Sahai, R.; Rillema, D. P.; Shaver, R.; Wallendael, S. V.; Jackman, D. C.; Boldaji, M. *Inorg. Chem.* **1989**, *28*, 1022.
(38) Rillema, D. P.; Callahan, R. W.; Mack, K. B. *Inorg. Chem.* **1982**, *21*, 2589.